Trunk Wormhole Detection using Bio-Impedance Spectroscopy Measurements: A Feasibility Study

Wei Wang1, Xiongxing Zhang1, Kening Wang1, Yuxiang Yang2

1 School of Optoelectronic Engineering, Xi'an Technological University, Xi'an, China
2 Department of Precision Instrumentation Engineering, Xi'an University of Technology, Xi'an, China

***Abstract* -- Stem-Boring Pest (SBP) cause the most prevalent problem that harms the health of trees. Traditional SBP prevention uses manual survey of wormholes and is a time-consuming process. This paper proposes a novel Trunk Wormhole Detection (TWD) method based on Bio-Impedance Spectroscopy (BIS) measurements. A horizontal and a vertical trunk wormhole phantoms are prepared, and comparative BIS measurements under the situations without and with holes are performed using a precision impedance analyzers WK6500B. Remarkable differences both on impedance amplitudes and phases have been found before and after the holes formed in the phantoms. The Cole model parameter analysis finds that the Cole parameter R∞ decreases by 43.82% in the horizontal phantom, and decreases by 63.13% in the vertical phantoms, which suggests that R∞ may be an efficient indicator to detect trunk wormholes.**

Keywords -- Trunk wormhole, Bio-impedance spectroscopy, Cole model

I. INTRODUCTION

Pest attacks have been one of the most harmful factors to the health of trees, and stem-boring pest (SBP) is the most prevalent problem [1]. Often, pest eggs are laid in the crevice of the stem bark by female pests, and then the hatched larvae will bore into the trunk and produce tunnels or wormholes, which would destroy the nutrient delivery channels and finally cause weakness or death of trees [2]. The difficulty of pest prevention and control is that pests live in a hidden world and are hardly to be discovered.

The early methods of SBP prevention are mainly based on manually looking for wormholes, such as the injection method [3], which refers to artificially injecting pesticide into wormholes to kill the larvae inside. However, this approach will waste time and energy in discover-ing wormholes manually according to external symptoms of barks.

In the last decade, modern technologies are adopted to detect trunk wormholes by researchers. In 2003, Cruvinel et al. used X-ray computerized tomography (CT) to detect wood damage by drilling holes into wood to simulate wormhole damage, and found that the location of wormhole can be identified on the images, but the contrast resolution of images was as low as 43.5% [4]. In 2009, Hussein et al. adopted bioacoustics features analysis to detected red palm weevil (RPW) larvae [5]. Experimental results showed that the existence of RPW larvae can be effectively detected through their feeding sound, but the extent of damage they made cannot be tested yet. In 2010, Siriwardena et al. developed a portable acoustic device to capture the acoustic sounds of the RPW larvae inside coconut palm stems [6]. Despite the convenience of this device, missing detection still exists because the pupil stage of pest will not produce sounds and therefore they might be left out.

Bio-impedance Spectroscopy (BIS) is one of the monitoring parameters for biological tissues based on multi-frequency and complex impedance measurement. In accordance with the law that the resistive and capacitive components of complex impedance vary remarkably with the changing of loading frequency, BIS method can obtain physiological and pathological states of biological tissues [7]. BIS technology is mainly used in diagnosis of human and animal diseases [8] and medical experiments [9]. In recent years, BIS technology has been applied in plant researches, such as detecting physiological states of plant [10], detection of plant diseases [11] and nutrient status [12], assessment of apple bruise [13, 14] and pine tree's freeze-thaw injury [15], etc. There-fore, wormhole, which dramatically changes the inner micro-structure and the conductive path of the trunk, has the possibility to be detected by its outer impedance characteristic.

This paper proposes a novel trunk wormhole detection (TWD) method based on BIS measurements. Two trunk wormhole phan-toms with a horizontal and a vertical hole respectively, are de-signed, and BIS measurement experiments are performed using a commercial impedance analyzers WK6500B. Then the experiment results (BIS data) have been fitted to the Cole model and the resultant model parameter changes are analyzed.

II. BIS MEASUREMENT EXPERIMENTS

A. Wormhole Phantoms Preparation

Two fresh flowering cherry trunks, both with the length of 140mm and diameter of 35mm, are selected as the horizontal and vertical wormhole phantoms, as shown in Fig. 1. On the horizontal phantom, two needle electrodes (using iron nails) are hammered into the trunk with the distance of 35mm along the longitudinal direction. On the vertical phantom, two needle electrodes are hammered along the radial direction. The profile of wormhole phantoms is shown in Fig. 2. For each trunk, the BIS measurement can be performed through the two electrodes. After the original (without hole) BIS data are collected, two holes with a diameter of 5mm and a depth of 15mm are drilled to simulate the wormholes, in which one hole is drilled radially at the middle of the two needle electrodes on the horizontal phantom, while another hole is drilled longitudinally at the circle core on the vertical phantom.

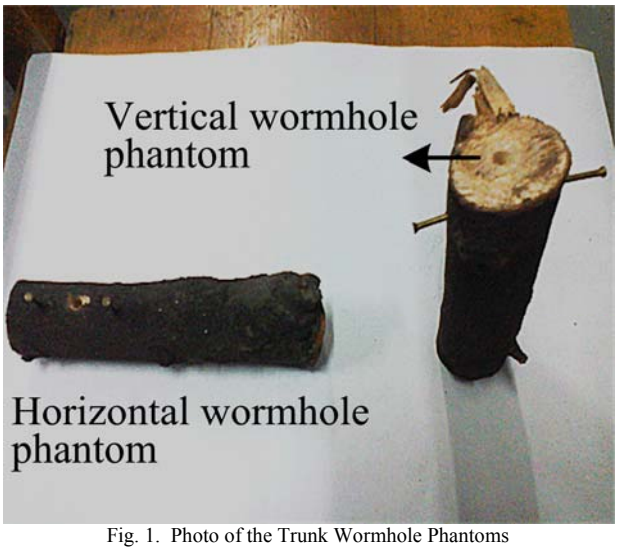

Fig. 1. Photo of the Trunk Wormhole Phantoms

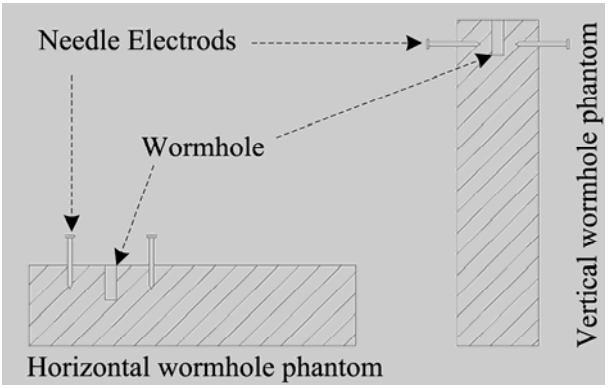

Fig. 2. Profile of the Trunk Wormhole Phantoms

B. BIS Measurement Experiments

The BIS measurement experiments on the two trunk wormhole phantoms were performed by a precision impedance analyzer WK6500B (WAYNE KERR Electronics Corp., UK). Two clamps derived from WK6500B were connected with the two needle electrodes of the tested phantom, as shown in Fig. 3. The sweeping frequency range of WK6500B was set linearly from 10 kHz to 800 kHz, and 791 points BIS data were obtain for each sweep-frequency measurement.

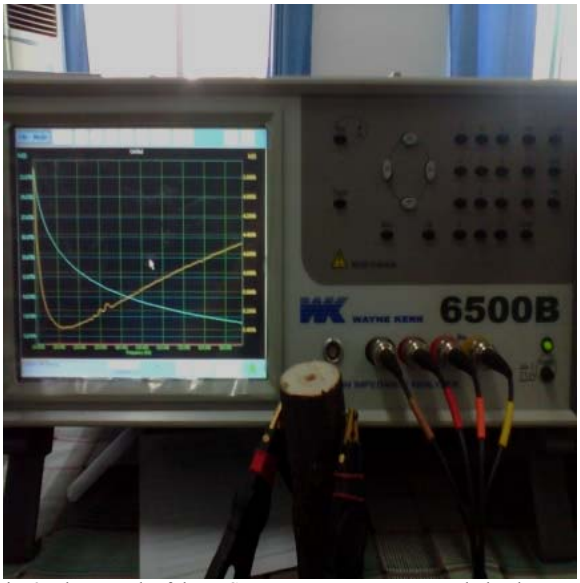

Fig. 3. Photograph of the BIS Measurements on a Wormhole Phan-tom by Precision Impedance Analyzer WK6500B

For each phantom, two times of BIS measurements, without hole and with hole, are performed. Finally, four sets of BIS data are obtained, namely, horizontal model without hole, horizontal model with hole, vertical model without hole and vertical model with hole. Fig. 4 shows the comparison of the BIS results of the two phantoms without and with hole, in which Fig. 4(a) and (b) exhibit the impedance amplitude-frequency and phase-frequency curves of the horizontal phantom respectively, while Fig. 4(c) and (d) illustrate those of the vertical phan-tom. From the four figures in Fig. 4, we can observe that there are obvious differences between the situations of without hole and with hole, both in impedance amplitudes and phases. The impedance amplitudes decline at the full frequency range after the hole is formed, while the impedance phases decline at the low frequencies and increase at the high frequencies.

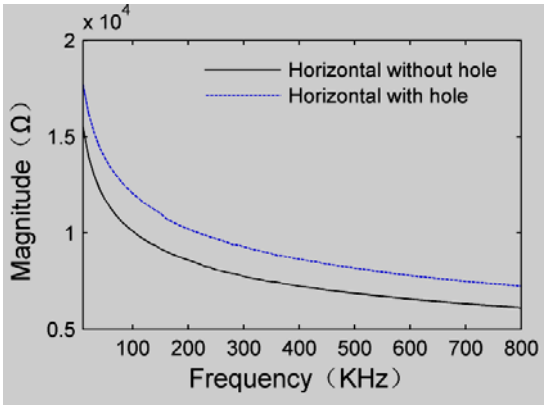

(a) Amplitude-frequency curves of horizontal phantom without and with hole

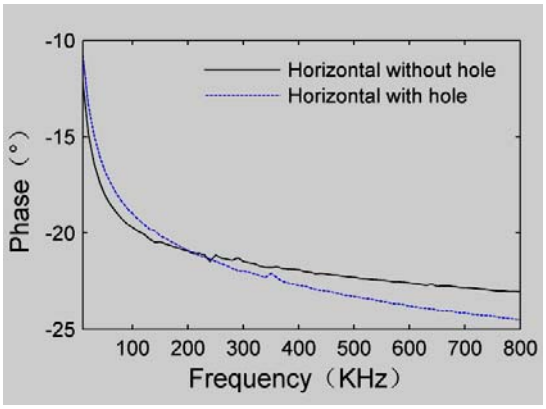

(b) Phase-frequency curves of horizontal phantom without and with hole

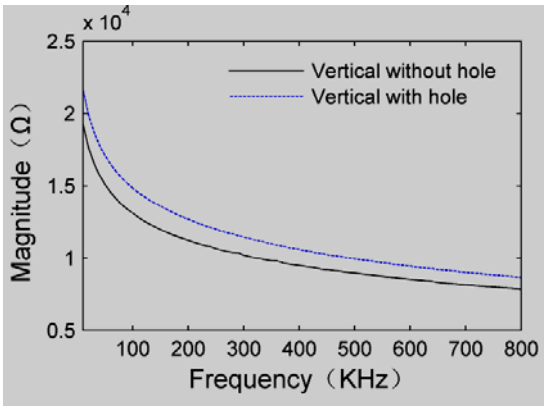

(c) Amplitude-frequency curves of vertical phantom without and with hole

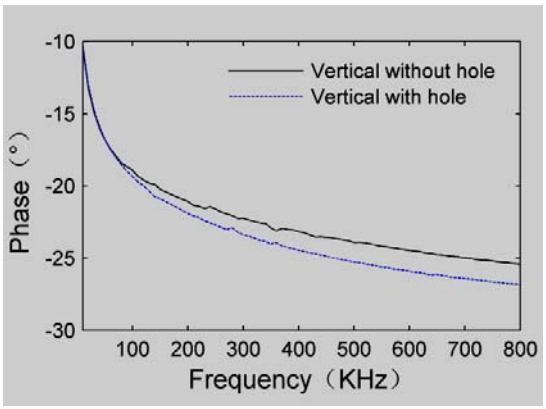

(d) Phase-frequency curves of vertical phantom without and with hole

Fig. 4. Amplitude-Frequency and Phase-Frequency Curves of Horizontal and Vertical Phantom without and with Hole

III. COLE MODEL PATAMETER ANALYSIS

A. Cole Model Method

The impedance a biological structure is normally obtained by measuring the real/resistive (R) and imaginary/reactive (X) components, the Cole function has been widely adopted for evaluating physiological or pathological status, which has been proposed by K.S. Cole in 1940 [16]. The Cole function is an empirically derived equation representing the tissue impedance within one dispersion in the form:

$$Z(\omega) = R_\infty + \frac{R_0 - R_\infty}{1 + (j\omega\tau)^\alpha} \quad (1)$$

where Z(ω) denotes the complex impedance at angular frequency ω and ω = 2π*f* (*f* = frequency), R0 is the resistance at zero frequency and R∞ the resistance at infinite frequency, α is an empirical exponent (dimensionless) with values between 0 and 1 as a measure of the position of the centre of the circle below the horizontal axis, τ is a characteristic time constant corresponding to a characteristic frequency *f*C (the frequency at which the reactance is maximum) [17],

$$f_C = \frac{\omega}{2\pi} = \frac{1}{2\pi\tau} \quad (2)$$

The Cole model then can be expressed as

$$Z(f) = R_\infty + \frac{R_0 - R_\infty}{1 + (j\frac{f}{f_C})^\alpha} \quad (3)$$

A typical Cole plot where the resistive part R (in horizontal axis) is plotted against the conjugate part of the reactance X (in vertical axis) is shown in Fig. 5, in which the fitted semicircle travels through the original measured data (hollow points) according to certain rules from right side to left side along the locus as the frequency *f* increased [16]. In Fig. 5, R0 and R∞ are the intersections of the arc and the horizontal (real) axis, and the semi-circle has an approximated radius (R0 –R∞)/2. α is a measure of

the position of the centre of the circle below the horizontal axis. fC is the frequency at which the reactance is maximum (the top of the semicircle).

The Cole parameters (R0, R∞, α and fC) are therefore the base of BIS data analysis, and fitting the complex BIS measurements data onto the Cole equation (1) and then extracting the Cole parameters become a common practice in BIS applications. This paper adopts the iterative least squares fitting algorithm proposed by Kun et al. [18] to extract Cole parameters R0, R□ and □, and makes a more reasonable modification on the calculation meth-od of τ.

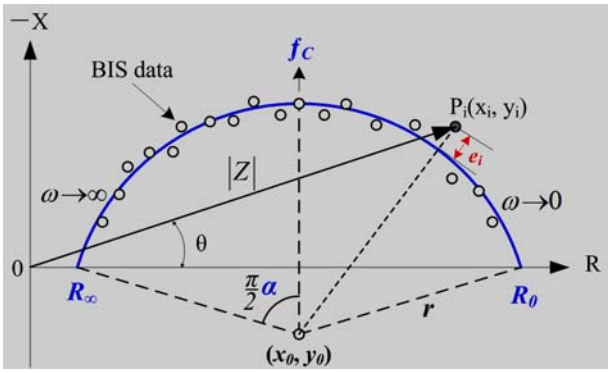

Fig. 5. Cole Plot

According to the Cole plot as shown in Fig. 5, the radial error ei is defined by the distance between the measured BIS data point Pi(xi, yi) and the fitted semicircle in the radial direction. The least square error function is the sum of squared ei at various frequencies (where i = 1 … m; m is the number of measurement frequencies):

$$F(x_0, y_0, r) = \sum_{i=1}^{m} e_i^2 = \sum_{i=1}^{m} \left(\sqrt{(x_i - x_0)^2 + (y_i - y_0)^2} - r \right)^2 \tag{4}$$

To determine the least square based optimal parameter set (x0, y0, r), the following system of equations should be fulfilled:

$$\begin{cases} \dfrac{\partial F}{\partial x_0} = 0 \\ \dfrac{\partial F}{\partial y_0} = 0 \\ \dfrac{\partial F}{\partial r} = 0 \end{cases} \tag{5}$$

These equations produce:

$$\begin{cases} \sum_{i=1}^{m} x_i - m x_0 - r \sum_{i=1}^{m} \dfrac{x_i - x_0}{\sqrt{(x_i - x_0)^2 - (y_i - y_0)^2}} = 0 \\ \sum_{i=1}^{m} y_i - m y_0 - r \sum_{i=1}^{m} \dfrac{y_i - y_0}{\sqrt{(x_i - x_0)^2 - (y_i - y_0)^2}} = 0 \\ \sum_{i=1}^{m} \sqrt{(x_i - x_0)^2 + (y_i - y_0)^2} - mr = 0 \end{cases} \tag{6}$$

The parameter set (x0, y0, r) in equation set (6) can be solved numerically using iterative methods:

$$\begin{cases} x_0^{(k+1)} = \dfrac{1}{m}\left[\sum_{i=1}^{m} x_i - r^{(k)} \sum_{i=1}^{m} \dfrac{x_i - x_0^{(k)}}{\sqrt{(x_i - x_0^{(k)})^2 - (y_i - y_0^{(k)})^2}} \right] \\ y_0^{(k+1)} = \dfrac{1}{m}\left[\sum_{i=1}^{m} y_i - r^{(k)} \sum_{i=1}^{m} \dfrac{y_i - y_0^{(k)}}{\sqrt{(x_i - x_0^{(k)})^2 - (y_i - y_0^{(k)})^2}} \right] \\ r^{(k+1)} = \dfrac{1}{m}\left[\sum_{i=1}^{m} \sqrt{(x_i - x_0^{(k)})^2 - (y_i - y_0^{(k)})^2} \right] \end{cases} \tag{7}$$

After the circle core (x0, y0) and radius r is fitted using BIS data, the Cole parameters R_0, R_∞ and α can be calculated analytically from x0, y0 and r, as:

$$R_0 = x_0 + \sqrt{r^2 - y_0^2} \tag{8}$$

$$R\infty = x_0 - \sqrt{r^2 - y_0^2} \tag{9}$$

$$\alpha = 1 - \frac{2}{\pi} \arcsin\left(\frac{|y_0|}{r} \right) \tag{10}$$

As for the fourth Cole parameter τ, this paper gives a more reasonable calculation method. According to equation (1), for every, τ has a concrete value at each BIS data point Pi(xi, yi):

$$\tau_i = \frac{\left(\dfrac{R_0 - Z_i(\omega_i)}{Z_i(\omega_i) - R_\infty} \right)^{\frac{1}{\alpha}}}{j\omega_i} \tag{11}$$

Where $Z_i(\omega_i)$ denotes the complex impedance at frequency ω_i : $Z_i(\omega_i) = x_i + jy_i$. Then the Cole parameter can be determined as the average of τ_i:

$$\tau = \frac{1}{m}\sum_{i=1}^{m} |\tau_i| = \frac{1}{m}\sum_{i=1}^{m} \frac{1}{\omega_i} \left| \left(\frac{R_0 - Z_i(\omega_i)}{Z_i(\omega_i) - R_\infty} \right)^{\frac{1}{\alpha}} \right| \tag{12}$$

Finally, the characteristic frequency fC can be computed according to equation (2).

B. Experiment Analysis Results

The obtained four sets of the BIS data are then fitted onto the Cole model based on the iterative least squares fitting algorithm mentioned above, and the resultant two sets of Cole plots comparison between the situations without hole and with hole are shown in Fig. 6(a) and (b). The Cole parameters (R0, R∞, α and τ) for each BIS set, and their rate of change, are listed in Table 1, among which R0 represents the resistance at zero frequency, R∞ refers the resistance at infinite frequency, and fC indicates the frequency where the reactance stays on the maximum, α (with values between 0 and 1) is a measure of the position of the center of the circle below the horizontal axis. From I, we can see that the Cole parameter R∞, the resistance at infinite frequency, decreases by 43.82% from 1380.98 Ω to 775.81 Ω in the horizontal phantom, and decreases by 63.13% from 343.47 Ω to 126.62 Ω in the vertical phantoms, after the hole is formed.

TABLE 1 COLE PARAMETERS AND THEIR CHANGE RATE COMPARISON BETWEEN THE SITUATIONS WITHOUT HOLE AND WITH HOLE

Cole Parameters	Horizontal phantom		Rate of change	Vertical phantom		Rate of change
	without hole	with hole		without hole	with hole	
R_0 (Ω)	23126.73	24885.61	7.6%	26844.40	29230.73	8.89%
R_∞ (Ω)	1380.98	775.81	-43.82%	343.47	126.62	-63.13%
fC (kHz)	32.95	58.73	78.24%	69.10	81.15	17.44%
α	0.41	0.40	-2.44%	0.40	0.42	5%

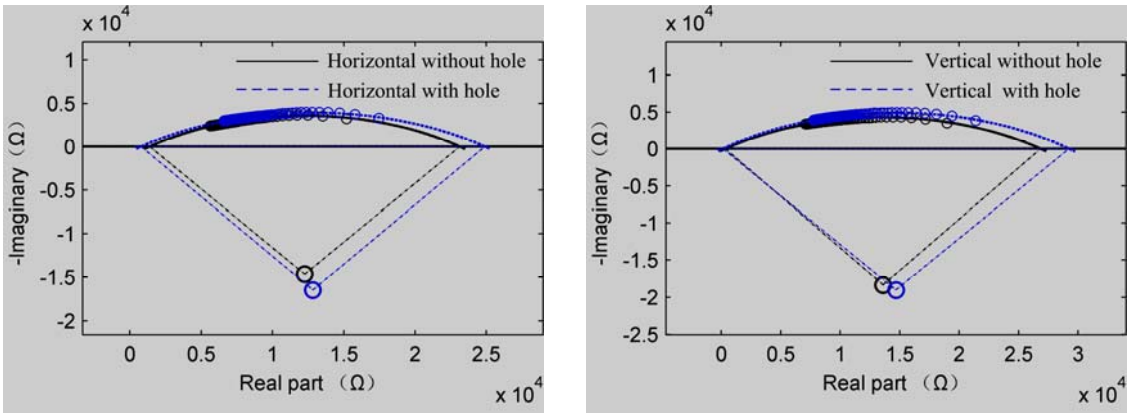

(a) Cole plots of horizontal phantom without and with hole (b) Cole plots of vertical phantom without and with hole

Fig. 6. Comparison of the Cole Plots between the Situations without and with Hole

IV. CONCLUSION

This paper proposes a novel trunk wormhole detection method based on bio-impedance spectroscopy (BIS) measurements. A horizontal and a vertical trunk worm-hole phantom are made, and comparative BIS measurement experiments are performed. Remarkable differences both on impedance amplitudes and phases have been found before and after the holes formed in the phantoms. Further, the Cole model parameter analysis finds that the Cole parameter R∞ decreases by 43.82% in the horizontal phantom, and decreases by 63.13% in the vertical phantoms after the holes formed, which suggests that R∞ may be an efficient indicator to detect trunk wormholes. This paper preliminarily validates the feasibility of trunk wormhole detection based on BIS measurements.

CONFLICT OF INTEREST

The authors confirm that this article content has no conflicts of interest.

ACKNOWLEDGMENT

This study has been partly supported by a grant from the National Natural Science Foundation of China. (No.61273271) and a grant from Natural Science Basic Research Plan in Shaanxi Province of China (No.2016JM6046).

REFERENCES

[1] B. E. Wichman, Forest Health in the Blue Mountains: The Influence of Insects and Diseases: USDA Forest Service, Pacific Northwest Research Station, 1992 (http://www7.nau.edu/mpcer/direnet/publications/publications_v/files/wickman-1992.pdf)..

[2] P. H. Yang, "Review of the Asian Longhorned Beetle Re-search, Biology, Distribution and Management in China," Food and Agriculture Organization of the United Nations, Rome, 2005 (ftp://ftp.fao.org/docrep/fao/012/j6355e/j6355e00.pdf).

[3] Q. Jian-guo, T. Fei-fei, Z. Yu-rui, K. Li-fen, and B. Rui-xia, "Effects of different methods on trunk-borers," Hebei Jour-nal of Forestry and Orchard Research, vol. 26, 2011.

[4] P. E. Cruvinel, J. d. M. Naime, M. Borges, Á. Macedoe, and A. Zhang, "Detection of Beetle Damage in Forests by X-ray CT Image Processing," R. Árvore, Viçosa-MG, vol. 27, pp. 747-752, 2003.

[5] W. B. Hussein, M. A. Hussein, and T. Becker, "Application of the signal processing technology detection of red palm weevil," in 17th European Signal Processing Conference (EUSIPCO 2009), Glasgow, Scotland, 2009.

[6] K. A. P. Siriwardena, L. C. P. Fernando, N. Nanayakkara, K. F. G. Perera, A. D. N. T. Kumara, and T. Nanayakkara, "Portable acoustic device for detection of coconut palms in-fested by Rynchophorus ferrugineus (Coleoptera: Curculio-nidae)," Crop Protection, vol. 29, pp. 25-29, 2010.

[7] S. Grimnes and Ø. G. Martinsen, Bioimpedance And Bioelectricity Basics. UK: Academic Press, 2008.

[8] G. Hornero, D. Diaz, and O. Casas, "Bioimpedance system for monitoring muscle and cardiovascular activity in the stump of lower-limb amputees," Physiological Measurement, vol. 34, pp. 189-201, Feb 2013.

[9] E. Okamoto, Y. Kato, S. Kikuchi, and Y. Mitamura, "Measurement of electrode-tissue interface impedance for im-provement of a transcutaneous data transmission using hu-man body as transmission medium," Biomed Mater Eng, vol. 24, pp. 1735-1742, Jan 1 2014.

[10] E. Borges, M. Sequeira, A. F. V. Cortez, H. C. Pereira, T. Pereira, V. Almeida, et al., "Assessment of Physiological States of Plants in situ-An Innovative Approach to the use of Electrical Impedance Spectroscopy," in BIOTECHNO 2013: The Fifth International Conference on Bioinformatics, Bio-computational Systems and Biotechnologies, Lisbon, Portu-gal, 2013.

[11] E. Borges, A. P. Matos, J. M. Cardoso, and C. Correia, "Ear-ly detection and monitoring of plant diseases by Bioelectric Impedance Spectroscopy," in 2012 IEEE 2nd Portuguese Meeting in Bioengineering (ENBENG), Coimbra, 2012, pp. 1-4.

[12] Greenham, C.G., P. J. Randall, and W. J. Muller, "Studies of phosphorus and potassium deficiencies in Trifolium subter-raneum based on electrical measurements," Canadian Jour-nal of Botany, vol. 60, pp. 634-644, 1982.

[13] M. A. Cox, M. I. N. Zhang, and J. H. M. Willison, "Apple bruise assessment through electrical impedance measure-ments," Journal of Horticultural Science, vol. 68, pp. 393-398, 1993.

[14] P. J. Jachson and F. R. Harker, "Apple Bruise Detection by Electrical Impedance Measurement," Hort Science, vol. 35, pp. 104-107, 2000.

[15] T. Repo, M. I. N. Zhang, A. Ryyppö, E. Vapaavuori, and S. Sutinen, "Effects of freeze-thaw injury on parameters of distributed electrical circuits of stems and needles of Scots pine eedlings at different stages of acclimation," Journal of Experimental Botany, vol. 45, pp. 823-833, 1994.

[16] S. C. Kenneth and H. C. Robert, "Dispersion and Absorption in Dielectrics I. Alternating Current Characteristics," The Journal of Chemical Physics, vol. 9, pp. 341-351, 1941.

[17] J. N. Bernt, T. Christian, G. M. Ørjan, and G. Sverre, "Evalu-ation of algorithms for calculating bioimpedance phase angle values from measured whole-body impedance modulus," Physiological Measurement, vol. 32, p. 755, 2011.

[18] S. Kun, B. Ristic, R. A. Peura, and R. M. Dunn, "Real-time extraction of tissue impedance model parameters for electri-cal impedance spectrometer," Medical & Biological Engi-neering & Computing, vol. 37, pp. 428-32, Jul 1999.